www.czasopisma.pan.pl PAN POLSKA AKADEMIA NAUK www.journals.pan.pl

A R C H I V E S O F M E T A L L U R G Y A N D M A T E R I A L S

Volume 59 2014 Issue 3

DOI: 10.2478/amm-2014-0149

M. WINNICKI*, T. PIWOWARCZYK*, A. MAŁACHOWSKA*, A. AMBROZIAK*

EFFECT OF GAS PRESSURE AND TEMPERATURE ON STEREOMETRIC PROPERTIES OF Al+Al_2O_3 COMPOSITE COATINGS DEPOSITED BY LPCS METHOD

WPŁYW CIŚNIENIA I TEMPERATURY GAZU NA WŁAŚCIWOŚCI STEREOMETRYCZNE POWŁOK KOMPOZYTOWYCH NANIESIONYCH METODĄ LPCS

The paper deals with effect of working gas pressure and temperature on surface stereometry of coatings deposited by low-pressure cold spray method. Examinations were focused on aluminium coatings which are commonly used to protect substrate against corrosion. A commercial Al spherical feedstock powder with admixture of Al_2O_3 (Al + 60wt.-% Al_2O_3), granulation -50+10 μm, was used to coat steel, grade S235JR. The deposited coatings were studied to determine their stereometry, i.e. roughness, transverse and longitudinal waviness, topography of surface and thickness as the functions of gas pressure and temperature. A profilometer and focal microscope were used to evaluate the stereometric properties. In order to reduce the number of variables, the remaining process parameters, i.e. shape and size of de Laval nozzle, nozzle-to-substrate distance, powder mass flow rate, linear velocity of spraying gun, were kept unchanged. The investigation confirmed influence of temperature and pressure on coating thickness as well as on the surface seterometry.

Keywords: Cold Spray, metal-matrix composite, roughness, waviness

W artykule przedstawiono wpływ ciśnienia i temperatury gazu roboczego na sterometrię powierzchni powłok nakładanych za pomocą niskociśnieniowej metody natryskiwania na zimno. Powłoki na podłożu stalowym S235JR zostały wykonane przy użyciu komercyjnie dostępnego proszku Al z dodatkiem Al_2O_3 (20% Al/80% Al_2O_3 wagowo) o granulacji <50 μm, zostały wykonane powłoki na podłożu stalowym S235JR. Następnie za pomocą profilometru i mikroskopu konfokalnego określono właściwości stereometryczne powłok takie jak chropowatość, falistość, topografię powierzchni oraz grubość w funkcji temperatury i ciśnienia gazu roboczego. W celu zminimalizowania ilości zmiennych pozostałe parametry procesu nie były zmieniane. Badania potwierdziły wpływ ciśnienia i temperatury gazu na stereometrię powierzchni.

1. Introduction

Cold Spray method is the newest among all known thermal spraying technologies. An essential difference between Cold Spray and other thermal methods consists in absence of high temperatures in the process. The heat input is strictly controlled and although the gas is preheated to obtain higher velocity due to the fact that the particle contact with gas is very short and the gas cools rapidly during expanding in nozzle the particles temperature remains well below their melting temperature. In contrast to traditional thermal spraying methods where the feedstock material in form of wire or powder should melt completely to ensure bonding, in cold spray the bonding is obtain thanks to the high particles velocity which is sufficient to cause plastic deformation even in solid state. The prevailing bonding theory claims that during the impact of particles the oxide layer is broken and removed by forming jet hence the contact between the metallic clean surfaces is possible. The other mechanism which has high contribution to adhesion is mechanical interlocking. The coating stereometry should then depend mostly on degree of particle deformation and hence on its impact velocity [1,2].

Oxidation degree of the coating depends solely on the oxidation of powder feedstock [3, 4]. Hence, oxidation sensitive material can be deposited without protective atmosphere, thus reducing costs essentially.

In cold spray technologies, a coating of metal or plastic is deposited using a powder with granulation of 1-150 μm [5, 6] and 50-250 μm [7, 8], respectively, which particles are accelerated to the velocity of 300 to 1,200 m/s [9] by compressed gas creating supersonic jet. Gases used in this method are: air, nitrogen or helium. Gas is brought to its working temperature at the very beginning of the process. As the special convergent/divergent nozzle is used (so called de Laval nozzle), decompressing gas achieves supersonic velocity.

The powder feedstock can be introduced axially into convergent part of the nozzle (in High Pressure Cold Spray method, HPCS) or radially into divergent part, just downstream the nozzle throat (in Low Pressure Cold Spray method, LPCS). As the name itself indicates, these two methods differ

* WROCŁAW UNIVERSITY OF TECHNOLOGY, 5 ŁUKASIEWICZA STR., 50-371 WROCŁAW, POLAND

each other, first and foremost in the pressure applied, but also in the point of heater location and in granulation of powder being used. In LPCS method, the pressure level ranges 0.3 to 1.0 MPa [10, 11]. The heater is placed inside the spraying gun and its power is usually not higher than 10 kW, while powder granulation is approximately 5-50 μm [5, 9, 10, 12]. This allows to reach the gas velocity at nozzle outlet up to about 700 m/s [9]. In contrast, HPCS method uses input pressure over 1 MPa [10,11] and additional heater, apart from the main unit located in the spraying gun, being an additional component of the power exceeding 30 kW, which causes that the heated up gas can reach velocity even up to 1,200 m/s [9]. The granulation of feedstock powder is from 1 to 150 μm [5].

For the sake of high energy of powder particles necessary to get bonding, the key parameters in cold spray method are identical to those in all thermal spraying methods, i.e. temperature and particle velocity. By steering these parameters, sufficiently high process energy can be attained to cause bonding the powder particles with substrate. In cold spraying, particles remains its solid state in gas jet, hence their high velocity is necessary, so as to brake thin film of oxides on the substrate and to connect with pure metals. This confirm theory that some minimum critical velocity v_c exists which provides sufficient kinetic energy E_k, when powder contacts substrate, to ensure its depositing [13]. Exceeding the critical velocity is directly related with attaining high productivity of the process, which translates into desirable thickness of the coating at low powder loss. Kinetic energy E_k of particle with the mass m_p and velocity $v_p \geqslant v_c$ will be as follows:

$$E_K = \frac{m_p \cdot v_p^2}{2}, \tag{1}$$

The maximum kinetic energy E_k attained at the moment when particle contacts substrate, is turned into several other quantities including: plastic strain energy E_p, elastic strain energy E_e, energy used to overcome friction E_f and thermal energy Q:

$$E_K = E_p + E_e + E_f + Q, \tag{2}$$

This leads to adiabatic shearing, the phenomenon which plays the main role in bonding the particles with substrate and with each other. Allowing additionally for fluctuations of stress, deformations, temperatures and also microstructures, local plastic flow happens there. As a result, a coating of high adherence is obtained.

Aluminium is often used in cold spray method due to its low mass and large ductility. Coatings made with this method are distinguished by high resistance to corrosion, close to that of pure aluminium, and by hardness higher than that of cold-rolled aluminium sheet [14]. This is due to the mechanism of powder particles bonding. Lower porosity of coating matters greatly in higher corrosion resistance. Lowered porosity is related to higher density of the coating, which can be attained by adding a ceramic phase.

Numerous advantages result from introducing ceramic phase into metal powder [10, 15]. As proved in [10], where Al powder was mixed with Al_2O_3, added ceramics caused the spraying productivity to increase by 30 up to 50% approximately. Additionally, as a result of compacting the ductile metal with hard phase, essentially lower porosity could be attain, from 30% for pure aluminium even down to 1% [10, 15]. Also the coating adhesion to substrate is thus increased even to 40-80 MPa [13] and likewise the hardness and abrasion resistance are improved [16].

According to the literature, thermal sprayed ceramic coatings are often analysed [17, 18]. However, there is no information about stereometry of Al-Al_2O_3 coatings, hence the examinations were focused on analysing the thickness, roughness and waviness of such coatings deposited by one spraying gun passage on commonly used S235JR steel.

2. Experimental Methods and Materials

The examinations carried out were centred around determining the roughness profile and waviness of coatings deposited by cold spray depending on the powder particle velocity applied. Powder was embedded on substrate by low-pressure cold spray unit, DYMET 413. Process parameters are given in Table 1. Commercially available spherical powder of aluminium with admixture of alumina (Al + 60wt.-% Al_2O_3) and granulation -50+10 μm (Fig. 1) was used in tests. Substrate was represented by 50×100 mm and 3 mm thick plate out of S235JR steel which chemical constitution is given in Table 2. Prior to spraying, the substrate subjected to grit blasting using alumina with particle granulation -350 μm as abrasive material at the pressure of 0.6 MPa. This way an oxide layer was removed and medium roughness Ra = 5.0 μm was attained. Compressed air was applied as the working gas. The scheme of shape for sprayed coating is shown in Fig. 2.

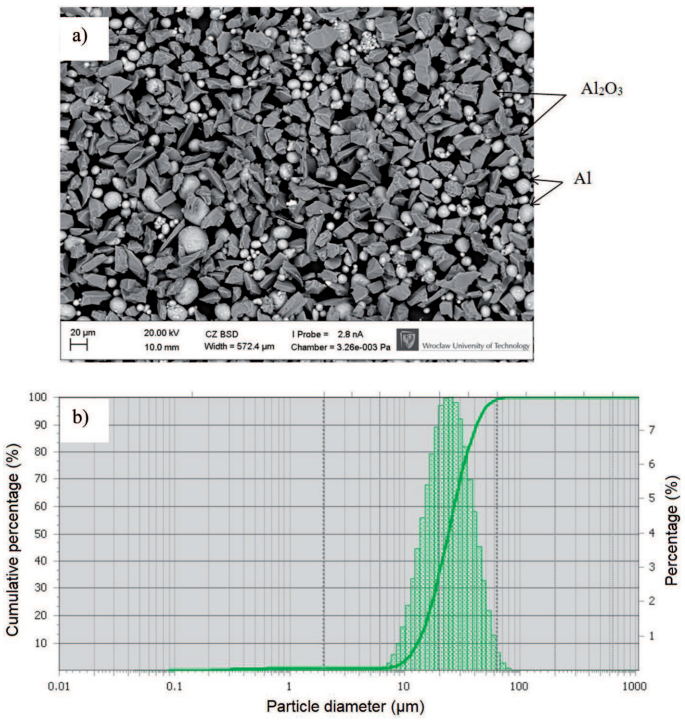

Fig. 1. SEM image (a) and distribution (b) of Al-Al_2O_3 powder

TABLE 1

Spraying parameters

	Spraying parameter					
	Gas pressure, MPa	Gas preheating temperature, K	Traverse speed, mm/s	Powder feeding rate, g/min	Standoff distance, mm	Number of layers
Value	0.5	573	10	40	20	1
	0.6					
		673				
	0.7					

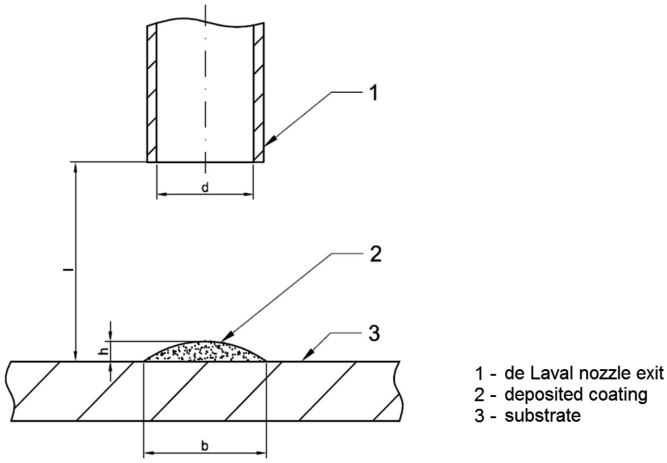

Fig. 2. Scheme of coating obtained by spraying with single pass of spraying gun

TABLE 2

Chemical constitution S235JR steel , % by weight (acc. to PN-EN 10025:2002)

C (max)	Mn (max)	P	S	N
0.2	1.4	0.045	0.045	0.009

The bead profile and its roughness are closely dependent on process parameters, i.e. mass flow rate of powder m_p, traverse speed linear velocity υ_l, temperature T_g and pressure p_g of working gas, type of working gas used (helium, nitrogen, air), powder granulation D_p and standoff distance from nozzle tip to substrate l. Some assumptions need to be adopted to determine the relation between coating stereometry versus pressure and temperature. Hence, all trials were carried out with round de Laval nozzle at constant distance from substrate of l = 20 mm, powder mass flow rate m_p = 40 g/min, spraying gun traverse speed υ_l = 10 mm/s and single pass of spraying gun along Y axis. It was found that the width of one bead for the nozzle diameter d = 5 mm, at spraying from the distance l = 20 mm is b = 7.4 mm, on an average.

Roughness and waviness were measured with stationary profilometer, Form Talysurf 120L, manufactured by Taylor Hobson, with measurement stylus terminated with diamond cone of apex angle 60° and corner radius r = 2 μm. The pressure exerted on diamond tip was 1 mN. There was also used the Nicon Eclipse LV150 microscope operated in reflected light, with CONFOCAM C101 module made by Confovis, creating inthe confocal system.

Evaluation of stereometric properties of deposited coatings was made according to the waviness of surface, *Wa*, and three basic features of roughness (acc. to PN-EN ISO 4287:1999 *Geometrical Product Specifications. Surface Texture – Profile Method. Terms, Definitions and Surface Texture Parameters)*:

Ra – arithmetic average of absolute values of ordinates $Z(x)$ inside elementary interval *lr*,

Rt – total height of roughness profile defined as the sum of the maximum peak height, *Zp* and the maximum depth of valley, *Zv* inside measuring interval, *ln,*

Rz (JIS) – ten point height of roughness profile, i.e. mean value of five absolute values of the largest peaks of the roughness profile and five largest valleys within elementary interval *lr*.

In the first stage of examinations, individual beads were made (3 for each trial) and their surface texture was determined: thickness *h*, roughness values *Ra, Rt, Rz*, and longitudinal waviness Wa_1. Then, coatings were deposited in five passes of spraying gun along axis X, at constant distance between bead axes equal to a =3.7 mm (Fig. 3), and examined were: thickness *h*, roughness values *Ra, Rt, Rz*, and transverse waviness Wa_2. Surface texture, thickness *h*, and transverse waviness Wa_2 were examined in 3 measurements at distances of 5 mm (measurement No. 1), 25 mm (measurement No. 2) and 45 mm (measurement No. 3) from perpendicular edge of sample, while roughness values *Ra, Rt, Rz* and longitudinal waviness Wa_1 – in one measurement over segment of 20 mm in the axis of single bead, and in axis of the third pass in case of the layer.

Eventually the influence of process parameter on alumina content in the coatings was also analysed. For this purpose SEM micrographs of the last bead of each coating with 1000-time magnification were taken. Performed pictures were analysed with ImageJ software and percentage alumina content was obtained.

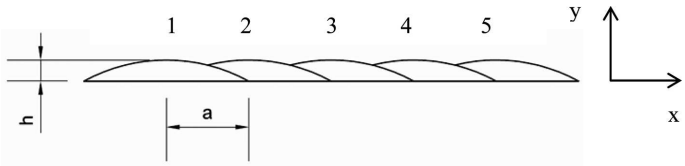

Fig. 3. Distribution scheme of coating with thickness *h* less than 1 mm obtained when spacing of spraying gun passes was a = 3.7 mm

3. Results and discussion

Examinations were carried out at variable parameters: temperatures of 573 and 673 K, and pressures within 0.5 to 0.7 MPa.

According to literature survey the pressure and temperature have the great impact on substrate sterometry and thickness as they influence the particles velocity. Additionally the temperature enhances thermal softening of particles thus facilitate their deformation [19, 20]. The thickness of copper coating tended to increase with higher gas pressure and tem-

perature. Although Goyal observed a sudden decrease in copper coating thickness while increasing temperature from 350 to 375 K. This was assigned to possibility of semi-melting of some particles [21]. Similar behaviour was observed in terms of roughness for copper coating [22].

The issue of melting may be even more important in case of aluminium as it had lower melting temperature than copper. The chosen temperatures and pressures for aluminium low-pressure cold spraying are well within the range given in literature: 0.6 MPa and 573 K [23], 0.5 MPa and temperature from 300 to 900 K, through form 800 K very high porosity was observed in the aluminum coatings [24], 0.7 MPa and 603 K [25].

Table 3 provides stereometric properties of coatings as single beads made after single passage of spraying gun for each trial. The lowest process efficiency was found for the first test at the lowest parameters. Created coatings were of thickness as low as about 50 μm and of low roughness as represented by *Ra* parameter of 4.6 μm and waviness of about 2.7 μm. Thickness of coatings in successive trial is over twice larger, even though the gas pressure was maintained at the same level and the temperature was just 100 K higher. At the same time, the basic roughness parameters and waviness of surface go higher. This rule is also valid for gas pressures 0.6 and 0.7 MPa, where temperature increase caused 2/3-times growth of coating thickness and distinct change in their roughness and surface waviness. Hence, we can explicitly state that, in case of low-pressure methods, increase of temperature causes change of coating thickness and development of its surface.

Similar relationship can be observed for constant temperature and variable gas pressure. When reviewing the trials 1-3-5 and 2-4-6, conclusions can be drawn that each time the pressure rises by 0.1 MPa, the coating thickness is 2/3 times higher and also a distinct change in roughness parameters and surface waviness are observed. Hence, we can come to the conclusion that higher pressure, being the key factor affecting particle velocity, is equally essential for the coating as increase of jet temperature causing additional heating of coating surface and plasticization of particles. Increase of temperature leads to change in stereometric properties, causing higher roughness and waviness.

When single layers were made, each time an upward tendency in their thickness was found in the initial stage of spraying. This is due to heating the nozzle from the flow of hot gas jet which leads to a change in conditions inside the nozzle. As a result, a gradual increase of coating thickness is observed. The results presented in the paper are those when the process was stabilized.

In order to verify the properties of stereometric beads, coatings were deposited in five passages of spraying gun along X axis (Table 4). Thickness of coating was taken for the highest bead in each measurement. Similarly to single coatings, here also a gradual increase of coating thickness for successive measurement was noted.

TABLE 3

Stereometric properties of single beads of coating

Trial No.	Process parameters		Roughness [μm]			Longitudinal waviness Wa_1 [μm]	Coating thickness h [μm]	
	Pressure p_1 [MPa]	Temp. T_1 [K]	*Ra*	*Rz* (JIS)	*Rt*		A	σ
1	0.5	573	4.6	15.9	43.4	2.7	48.3	3.4
2	0.5	673	5.9	19.5	53.6	5.6	104.4	7.9
3	0.6	573	5.0	17.5	45.9	2.9	97.8	5.4
4	0.6	673	7.7	23.1	67.4	11.2	301.7	64.3
5	0.7	573	8.3	24.0	86.4	9.0	296.7	20.5
6	0.7	673	11.0	27.1	108.7	13.7	558.9	97.5

A – Average ; σ – Standard deviation

TABLE 4

Stereometric properties of deposited coatings

Trial No.	Roughness [μm]			Longitudinal waviness Wa_1 [μm]	Transverse waviness Wa_2 [μm]		Coating thickness h [μm]		Alumina content [%]
	Ra	*Rz* (JIS)	*Rt*		A	σ	A	σ	
1	8.1	21.9	63.2	7.5	24.9	5.1	306.7	20.8	36.9
2	8.6	22.2	69.0	9.1	45.7	0.9	466.7	23.1	27.2
3	8.8	25.2	74.4	9.1	39.6	4.2	468.3	23.6	29.8
4	10.8	25.6	88.5	15.6	56.8	2.6	911.7	20.2	26.6
5	10.1	25.4	78.3	13.0	42.2	8.7	583.3	30.6	28.7
6	11.9	28.2	91.6	21.2	71.3	2.3	1078.3	43.7	24.1

A – Average ; σ – Standard deviation

It was observed that for two initial passages of the spraying gun, bead thickness continually increases until it reaches some regular value during the third passage. This is due to spraying gun heating by hot gas flowing through de Laval nozzle causing that the conditions in the nozzle varies. Additionally, for three initial passages, which last 40.8 s, for linear velocity of 10 mm/s, the substrate is gradually heated up due to gas and particles temperature, causing increase of coating thickness and, as proved in [26], heating up the substrate leads to higher process efficiency. Furthermore, despite the distance between successive spraying gun passages a = 3.7 mm, the beads overlap each other and when coating is sprayed in the next spraying gun passage, powder is deposited also on the previous bead. What is interesting, together with heating up the spraying gun and the substrate, the surface waviness keeps at similar level or even decreases.

The microstructure of the Al+Al_2O_3 coatings deposited by LPCS in trials 1 and 6 were investigated by SEM. The last beads of the coatings, the fifth ones, are shown in Figs 4 and 5. The darker grey particles visible in the photographs are the Al_2O_3 phase and the black points are pores. For clearer observation all the specimens were etched prior to examination. In the coatings deposited with lower process parameters (Fig. 4) there is a larger amount of pores than in the coatings deposited with lower process parameters (Fig. 5). Despite the high temperature (673 K) used in the process, the aluminium coating (Fig. 5) does not show much oxidation. The mean thickness of the Al+Al_2O_3 coatings deposited in trial 1 and 6 were amounted to 306.7 μm and 1078.3 μm, respectively. The presence of alumina ensures high density and minimizes the presence of pores. However it is higher temperature that makes aluminium plastic and ensures more uniform coating. In the case of the Al+Al_2O_3 coating deposited in trial 1, agglomeration of alumina particles were discovered (Fig. 4b). The continuous ceramic phase may make the coating vulnerable to brittle fracture.

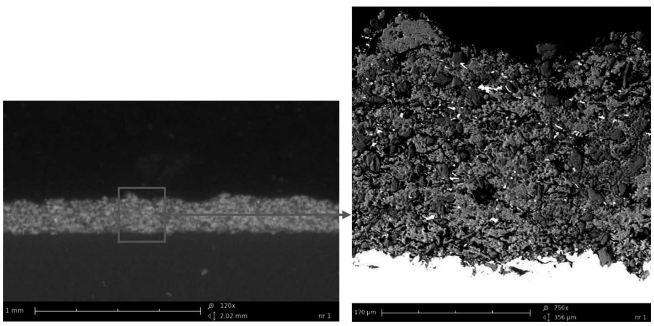

Fig. 4. SEM microstructure of LPCS Al+Al_2O_3 coating on S235JR deposited in trial 1

The analysis of alumina content shows that in the coating is much less alumina compared to the sprayed powder admixture, containing 60wt.-% of Al_2O_3. What is more coatings deposited with higher parameters contain less alumina. In this case the key parameter is temperature. The higher temperature the less alumina particles in the picture. Higher process parameters gives thicker coating, more metal particles is deposited and the alumina distribution is uniform. Moreover particles sprayed with low pressure and temperature gives coating with local aluminium agglomerations. Coating obtained in trial no. 1 (Fig. 4) was very thin, built with small Al particles and contain a lot of small Al_2O_3 particles. Thicker coating (Fig. 5) shows regular and uniform alumina distribution.

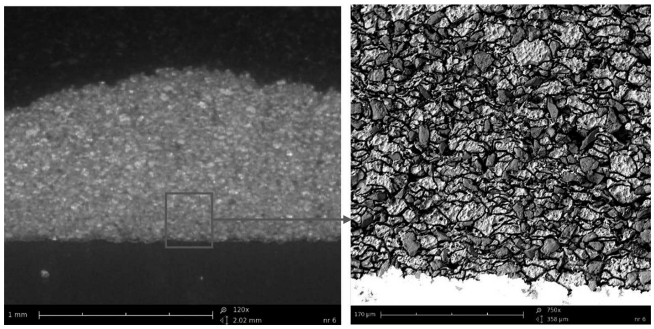

Fig. 5. SEM microstructure of LPCS Al+Al_2O_3 coating on S235JR deposited in trial 6

Figure 6a illustrates the top view of the thickest coating made in trial 6. Increase of temperature is of much higher effect on the coating thickness than that of pressure increase. Though the process is run under constant condition, higher gas temperature much more contributes to higher efficiency, not only by higher velocity and also by heating up the substrate which translates to higher coating thickness. Moreover powder softening in the spraying jet is also an effect of gas temperature. In cold spraying method the softer material is used the higher spraying efficiency is got. Besides, SEM images shows (Figs 4b vs. 5b) that coatings deposited with higher temperature are denser and contain less pores. Thermal softening makes aluminium more plastic so particles are deposited more uniformly in the coating due to plastic strain. It should be also noted that ceramic particles in the coating decrease heat flow what gives higher thermal energy during particle deposition.

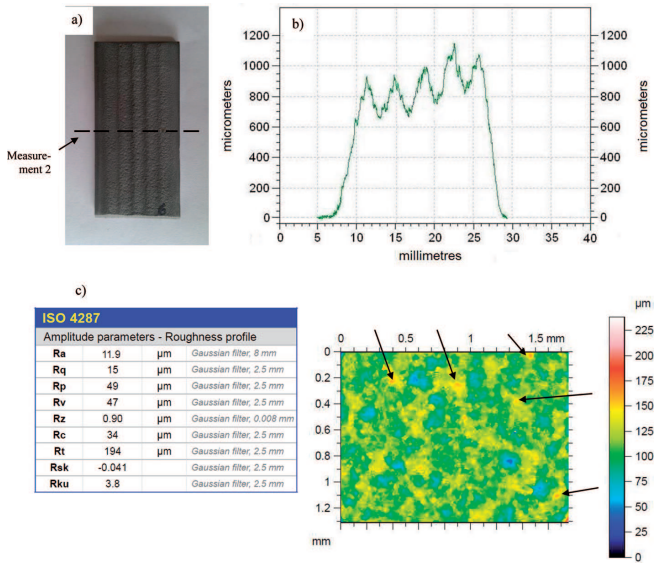

Fig. 6. Coating for trial 6: view of deposited coating (a), surface topography for measurement 2 (b), surface roughness from confocal microscope (c)

Exemplary topography of coating surface for trial 6 is shown in Fig. 6b. According to Table 4, there are essential differences in transverse waviness of the coating. For all trials, at temperature 573 K, it is almost twice lower than at higher

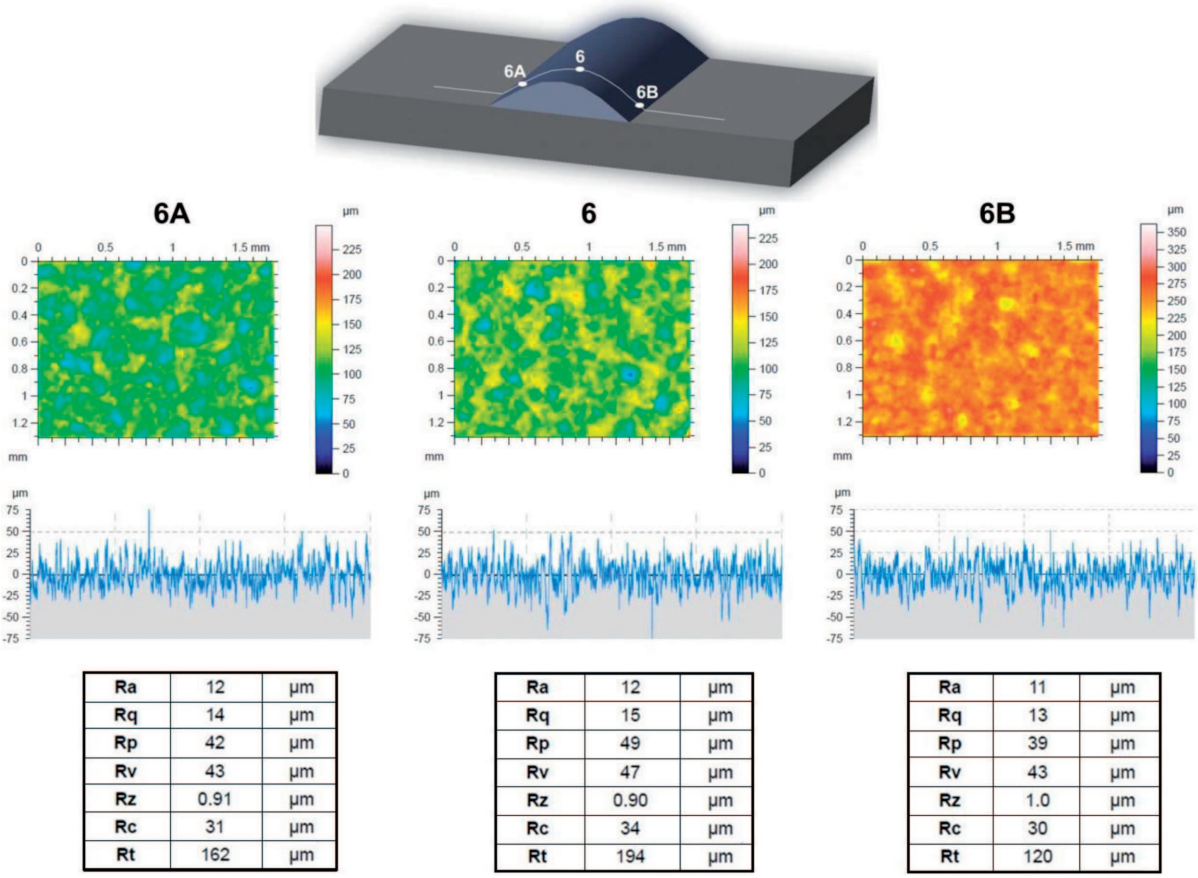

Ra	12	µm
Rq	14	µm
Rp	42	µm
Rv	43	µm
Rz	0.91	µm
Rc	31	µm
Rt	162	µm

Ra	12	µm
Rq	15	µm
Rp	49	µm
Rv	47	µm
Rz	0.90	µm
Rc	34	µm
Rt	194	µm

Ra	11	µm
Rq	13	µm
Rp	39	µm
Rv	43	µm
Rz	1.0	µm
Rc	30	µm
Rt	120	µm

Fig. 7. Roughness measurements with confocal microscope for three bead points

temperature of 673 K where its maximum value reaches 71.3 μm. Similar relationship exists for longitudinal waviness of coatings, however the values are considerably lower and range 7.5-21.2 μm. This is due to process irregularity caused by gravity feeding the powder. In contrast, surface roughness is somewhat higher than that of individual beads.

The degree of coating development is shown in photo from confocal microscope (Fig. 6c). Attention shall be drawn to the difference in thickness which was even 175 μm for trial 6. Figure 6c shows also, as pointed out by arrows, the powder particles deposited in the highest points of the coating. High roughness caused by uneven distribution of powder particles is an integral part of coating deposition with all thermal methods.

In order to verify the differences in roughness parameters across the layers, two additional measurements (6A and 6B) were made as close as possible the coating-substrate border with confocal microscope – Fig. 7. The measurement was taken in the middle of coating length, at distance of 25 mm from sample edge. It can be explicitly stated that independently of the measurement point (6, 6A, 6B), stereometric properties of the coating over its full cross-section are similar.

Figure 8 shows changes of basic roughness profiles, *Ra*, *Rz* and *Rt* versus gas pressure (p = 0.5÷0.7). Measurements were taken for two selected gas temeratures, 573 and 673 K. Both individual beads (a, b) and individual coatings (c, d) were measured. Clear increasing trend for all roughness profiles along with rising the gas pressure and (in lower degree) with gas temperature should be noted. Hence, it is possible to change the stereometric properties of deposited coatings by proper selection of basic process parameters.

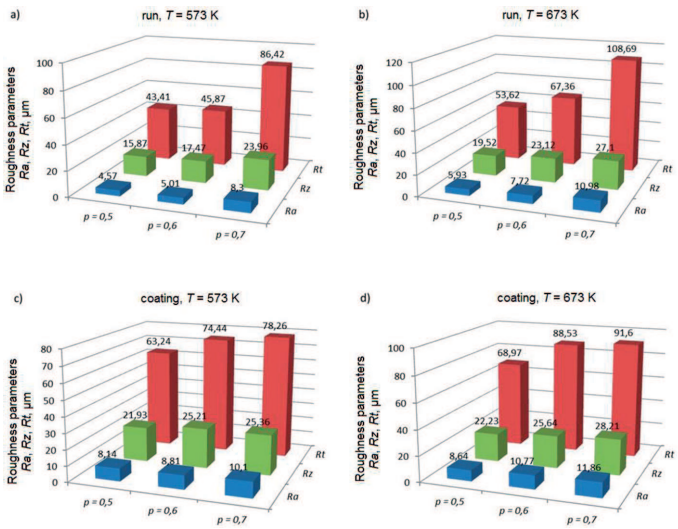

Fig. 8. Roughness parameters, *Ra*, *Rz* and *Rt* of beads and coatings versus gas pressure p for two gas temperatures: 573 K (a, c) and 673 K (b, d)

In connection with considerable differences in thickness of three initial beads of the coating, a verification trial was run for the highest parameters, i.e. pressure of 0.7 MPa and temperature of 673K. This time, the coating was deposited in 12 passes along axis X (Fig. 9a). Arrows point out the starting

points of the first and the last bead. A notable difference in the quantity of power deposited in these spots can be noted which translates into the coating thickness. The distribution profile for the measurement 2 is shown in Fig. 9b while the results of thickness measurements are summarized in Table 5.

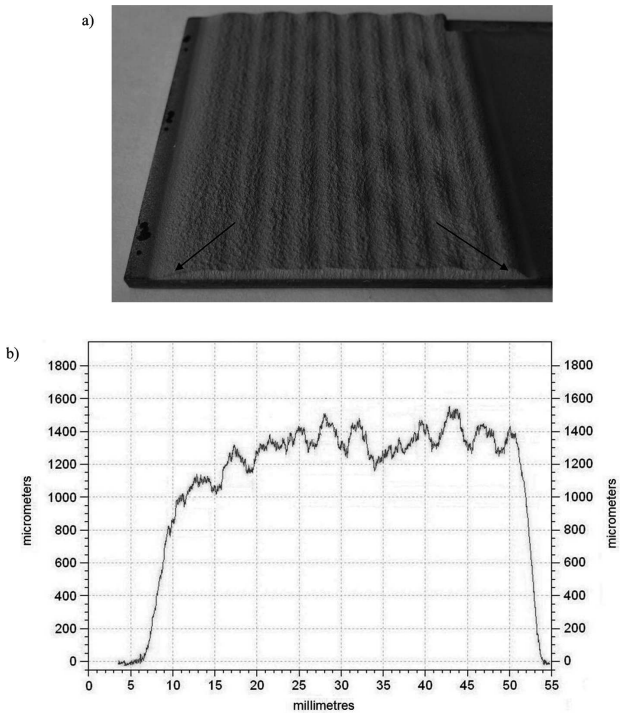

Fig. 9. Verification coating deposited in 12 spraying gun passes: view of deposited coating (a), profile distribution of verification coating for measurement 2 (b)

TABLE 5
Measurement of coating thickness for verification trial

Run No.	Coating thickness h [μm]	
	A	σ
1	1005.0	149.9
2	1162.7	108.1
3	1303.3	83.4
4	1405.0	76.7
5	1436.7	76.9
6	1408.3	78.1
7	1415.0	69.8
8	1396.7	73.9
9	1430.0	74.5
10	1488.3	85.3
11	1473.3	78.8
12	1355.0	61.4

A – Average; σ – Standard deviation

As can be seen, the mean thickness of the coating was 1.357 μm. The coating is distinguished by large transverse waviness reaching 79.4 μm, which is close to that of trial 6. There is also considerable increase of longitudinal waviness amounting to 57.6 μm which could be from stronger temperature effect. Roughness, according to the former trial, was 11.7 μm. As it can be noted from average values of thickness for each individual bead shown in Table 4, not until the third bead the thickness stabilizes itself, so in further part the distribution is similar.

4. Conclusions

Upon reviewing the results from examinations, the following conclusions can be drawn:

1. Direct relationship between pressure and temperature on one side and the thickness of deposited coating on the other side. Higher pressure allows the particles to exceed the critical velocity and to deposit them on substrate. Temperature affects the process in two ways: it increases the velocity of jet and heats up substrate and particles, thus causing higher efficiency of the process. This results in better quality of coating as it is dense and free of pores.
2. A gradual increase of coating thickness in three initial beads until the process stabilizes was observed. It is due to the effect of gas temperature. Within the first seconds of the process, de Laval nozzle heats up, so the conditions inside the nozzle changes and higher temperature inside the nozzle causes the gas jet velocity particle to increase. Then, the substrate and the coating already deposited also heat up which supports deposition of successive beads.
3. Coatings of higher thickness feature higher roughness and waviness of surface, which results from high parameters of the process, i.e. pressure and temperature. It should be emphasized that the examinations were made for Al powder with Al_2O_3 admixture. Alumina features particles with high hardness and irregular shape, which causes compacting and cratering the coating. Furthermore, uneven deposition of Al particles causes additional increase of surface roughness.
4. Higher waviness was observed along the beads. This is due to irregular course of the process caused by gravity feeding of the powder.

Acknowledgements

The paper comes into existence thanks to examinations financed by National Science Centre within the Project No. 2011/01/N/ST8/04975, entitled “Adhesive properties of various material coatings deposition with low-pressure cold spraying”.

REFERENCES

[1] T. Stoltenhoff, H. Kreye, H.J. Richter, An Analysis of the Cold Spray Process and Its Coatings, Journal of Thermal Spray Technology **11**(4), 542-550 (2002).
[2] T. Hussain, D.G. McCartney, P.H. Shipway, D. Zhang, Bonding Mechanisms in Cold Spraying: The Contributions of Metallurgical and Mechanical Component, Journal of Thermal Spray Technology **18**(3), 365-379 (2009).
[3] W.-Y. Li, Ch.-J. Li, H. Liao, Significant influence of particle surface oxidation on deposition efficiency, interface microstructure and adhesive strength of cold-sprayed copper coatings, Applied Surface Science **256**, 4953-4958 (2010).
[4] K.C. Kang, S.H. Yoon, Y.G. Ji, C. Lee, Oxidation Effects on the Critical Velocity of Pure Al Feedstock Deposition in the Kinetic Spraying Process, Thermal Spray 2007: Global Coating Solutions (ASM International), 66-71 (2007).

[5] R.Gr. Maev, S. Titov, V. Leshchynsky, D. Dzhurinskiy, M. Lubrick, In Situ Monitoring of Particle Consolidation During Low Pressure Cold Spray by Ultrasonic Techniques, Journal of Thermal Spray Technology **20** (4), 845-851 (2011).

[6] L. Ajdelsztajn, B. Jodoin, G.E. Kim, J.M. Schoenung, Cold Spray Deposition of Nanocrystalline Aluminum Alloys, Metallurgical and Materials Transactions A **36A**, 657-666 (2005).

[7] A.S. Alhulaifi, G.A. Buck, and W.J. Arbegast, Numerical and Experimental Investigation of Cold Spray Gas Dynamic Effects for Polymer Coating, Journal of Thermal Spray Technology, 2012, In Press.

[8] Y. Xu, I.M. Hutchings, Cold spray deposition of thermoplastic powder, Surface & Coatings Technology **201**, 3044-3050 (2006).

[9] K. Ogawa, K. Ito, K. Ichimura, Y. Ichikawa, S. Ohno, N. Onda, Characterization of Low-Pressure Cold-Sprayed Aluminum Coatings, Journal of Thermal Spray Technology **17** (5-6), 728-735 (2008).

[10] E. Irissou, J.-G. Legoux, B. Arsenault, Ch. Moreau, Investigation of Al-Al_2O_3 Cold Spray Coating Formation and Properties, Journal of Thermal Spray Technology **16** (5-6), 661-668 (2007).

[11] H. Koivuluoto, P. Vuoristo, Effect of Powder Type and Composition on Structure and Mechanical Properties of Cu +Al_2O_3 Coatings Prepared by using Low-Pressure Cold Spray Process, Journal of Thermal Spray Technology **19** (5), 1081-1092 (2010).

[12] M. Fukumoto, H. Wada, K. Tanabe, M. Yamada, E. Yamaguchi, A. Niwa, M. Sugimoto, M. Izawa, Deposition Behavior of Sprayed Metallic Particle on Substrate Surface in Cold Spray Process, International Thermal Spray Conference and Exposition, 2007, Beijing.

[13] P.C. King, G. Bae, S.H. Zahiri, M. Jahedi, Ch. Lee, An Experimental and Finite Element Study of Cold Spray Copper Impact onto Two Aluminum Substrates, Journal of Thermal Spray Technology **19** (3), 620-634 (2010).

[14] Q. Wang, N. Birbilis, M.-X. Zhang, Interfacial structure between particles in an aluminum deposit produced by cold spray, Materials Letters **65**, 1576-1578 (2011).

[15] A. Shkodkin, A. Kashirin, O. Klyuev, T. Buzdygar, Metal Particle Deposition Stimulation by Surface Abrasive Treatment in Gas Dynamic Spraying, Journal of Thermal Spray Technology **15** (3), 382-386 (2006).

[16] K. Spencer, D.M. Fabijanic, M.-X. Hang, The use of Al-Al2O3cold spray coatings to improve the surface properties of magnesium alloys, Surface & Coatings Technology **204**, 336-344 (2009).

[17] A. Pawlowski, T. Czeppe, W. Baliga, L. Górski, M. Faryna, The morphology of the Al_2O_3 - SiO_2 layer plasma sprayed onto a metallic substrate after heat treatment, Archives of Metallurgy and Materials **53**, 4, 985-992 (2008).

[18] A. Pawlowski, J. Morgiel, M. Faryna, L. Górski, J. Grzonka, Structure analysis of the plasma sprayed Al_2O_3 - SiO_2 coating on metallic substrate, Archives of Metallurgy and Materials **53**, 3, 679-682 (2008).

[19] H. Lee, H. Shin, S. Lee, K. Ko, Effect of gas pressure on Al coatings by cold gas dynamic spray, Materials Letters **62**, 1579-1581 (2008).

[20] J. Lee, S. Shin, H.J. Kim, C. Lee, Effects of gas temperature on critical velocity and deposition characteristics in kinetic spraying, Applied Surface Science **253** (7), 3512-3520 (2007).

[21] T. Goyal, R.S. Walia, T.S. Sidhu Study of Coating Thickness of Cold Spray Process Using Taguchi Method, Materials and Manufacturing Processes **27** (2), 185-192 (2012).

[22] T. Goyal, R.S. Walia, T.S. Sidhu, Surface roughness optimization of cold-sprayed coatings using Taguchi method, The International Journal of Advanced Manufacturing Technology **60** (5-8), 611-623 (2012).

[23] V. Champagne, D. Helfritch, Electromagnetic Interference Shielding by the Cold Spray Particle Deposition of an Aluminum – Alumina Matrix, Journal of Advanced Materials **40** (1), 20-26 (2008).

[24] A. Shkodki, A. Kashirin, O. Klyue, T. Buzdygar, Metal Particle Deposition Stimulation by Surface Abrasive Treatment in Gas Dynamic Spraying, Journal of Thermal Spray Technology **15**(3), 382-386 (2006).

[25] H.Y. Lee, S.H. Jung, S.Y. Lee, Y.H. You, K.H. Ko, Correlation between Al2O3 particles and interface of Al-Al2O3 coatings by cold spray, Applied Surface Science **252**, 1891-1898 (2005).

[26] S. Rech, A. Trentin, S. Vezzu, J.-G. Legoux, E. Irissou, and M. Guagliano, Influence of Pre-Heated Al 6061 Substrate Temperature on the Residual Stresses of Multipass Al Coatings Deposited by Cold Spray, Journal of Thermal Spray Technology **20**, 1-2, 243-251 (2011).

Received: 10 January 2014.